Imaging of hemoglobin oxygen saturation variations in single vessels *in vivo* using photoacoustic microscopy

Hao F. Zhang, Konstantin Maslov, and Mathangi Sivaramakrishnan
Optical Imaging Laboratory, Department of Biomedical Engineering, Texas A&M University, 3120 TAMU, College Station, Texas 77843-3120

Gheorghe Stoica
Department of Veterinary Pathobiology, Texas A&M University, College Station, Texas 77843-5547

Lihong V. Wang[a)]
Optical Imaging Laboratory, Department of Biomedical Engineering, Texas A&M University, 3120 TAMU, College Station, Texas 77843-3120

Photoacoustic microscopy was used to noninvasively image variations in hemoglobin oxygen saturation (SO$_2$) in the subcutaneous microvasculature of rats *in vivo*. In phantom tests, the calculated concentration fractions of red ink in double-ink mixtures matched the actual values with a 1% error. In *ex vivo* studies, the calculated SO$_2$ in bovine blood agreed with the standard spectrophotometric measurements within a 4% systematic difference. In *in vivo* studies, arteries and veins were separated based on the measured SO$_2$ values and variations in SO$_2$ between different physiological states (hyperoxia, normoxia, and hypoxia) were imaged in single blood vessels. © *2007 American Institute of Physics*. [DOI: 10.1063/1.2435697]

Imaging hemoglobin oxygen saturation (SO$_2$) is important for understanding brain hemodynamics in response to sensory stimulations.[1] It is also invaluable for numerous medical applications, such as evaluating the effects of chemotherapy and radiotherapy on tumors,[2] monitoring the healing of wounds,[3] and studying gene expression.[4] However, SO$_2$ has not been routinely imaged due to the existing noninvasive methods' lack of either spatial resolution or sensitivity. Current techniques that show potential for SO$_2$ imaging include near-infrared spectroscopy (NIRS), blood-oxygen-level-dependent (BOLD) contrast magnetic resonance imaging (MRI), electron paramagnetic resonance imaging (EPRI), positron emission tomography (PET), and single photon emission tomography (SPET). NIRS measures diffuse light at different wavelengths and calculates the SO$_2$ based on spectral measurements and the molar extinction differences between deoxyhemoglobin (HbR) and oxyhemoglobin (HbO$_2$). However, it suffers from poor spatial resolution because of the strong optical scattering in biological tissues. Although BOLD MRI can provide high spatial resolution, it is only sensitive to HbR and has trouble distinguishing between changes in oxygenation levels and changes in blood flow.[4] Because it is unable to image intrinsic contrast, EPRI requires the injection of potentially toxic free-radical contrast agents. PET and SPET require the intravenous administration of radioactive isotopes, and both have poor spatial resolution.

Photoacoustic microscopy[5–9] (PAM) is a high-resolution functional modality that images optical absorption contrast based on ultrasonic detection through the photoacoustic (PA) effect. It detects the emitted acoustic waves that result from short-pulsed laser-induced transient thermoelastic expansion when the incident optical energy is absorbed and transformed into heat.[10–13] If an ultrasonic detector with high central frequency, large bandwidth, and large numerical aperture is employed, the PA sources can be localized with high spatial resolution to image the internal optical absorption distribution. Since HbR and HbO$_2$ are two of the major optical absorbers in tissues, PAM is well suited to the imaging of blood vessels within an appropriate spectral region. Based on only endogenous contrast, PAM can reach a signal-to-background contrast of 3500% with high sensitivity and specificity *in vivo*.[8] PAM provides better spatial resolution than NIRS by taking advantage of ultrasonic detection, and it provides higher sensitivity than MRI due to high physiologically specific optical absorption contrast.

In this letter, we report on using PAM *in vivo* to image dynamic SO$_2$ variations in single subcutaneous vessels under three physiological states: hyperoxia, normoxia, and hypoxia. Prior to the *in vivo* study, the PAM system was tested by (1) calculating the concentration fraction of red ink in double-ink (blue and red inks) solutions and (2) comparing the SO$_2$ values from PAM measurements with values acquired by a standard optical method using bovine blood samples *ex vivo*.

To focus on the imaging of dynamic SO$_2$ variation here, we skip the explanations for the instruments and the imaging procedure of PAM. However, readers are referred to our previous works for details.[6–9]

PAM measures SO$_2$ in the same way NIRS does,[14] where HbR and HbO$_2$ are treated as the dominant absorbing compounds at each wavelength (λ_i). Thus the blood absorption coefficient $\mu_a(\lambda_i)$ (cm^{-1}) can be expressed as

$$\mu_a(\lambda_i) = \varepsilon_{\mathrm{HbR}}(\lambda_i)[\mathrm{HbR}] + \varepsilon_{\mathrm{HbO}_2}(\lambda_i)[\mathrm{HbO}_2], \qquad (1)$$

where $\varepsilon_{\mathrm{HbR}}(\lambda_i)$ and $\varepsilon_{\mathrm{HbO}_2}(\lambda_i)$ are the known molar extinction coefficients (cm^{-1} M^{-1}) of HbR and HbO$_2$ at wavelength λ_i, respectively, and $[\mathrm{HbR}]$ and $[\mathrm{HbO}_2]$ are the concentrations of the two forms of hemoglobin, respectively. Since the amplitude of the acquired localized PA signal $\phi(\lambda_i, x, y, z)$ is proportional to the local optical energy deposition, we can re-

---

[a)]Author to whom correspondence should be addressed; present address: Department of Biomedical Engineering, Washington University in St. Louis; electronic mail: lhwang@biomed.wustl.edu
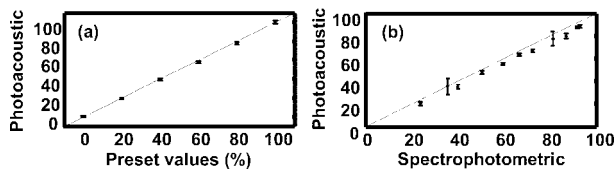
FIG. 1. (a) PAM measurements of the fraction of the red ink concentration in a mixture of red and blue inks ([Red]/[Red]+[Blue]). (b) Comparison of PAM measurements with spectrophotometric measurements of SO_2 in *ex vivo* bovine blood samples.
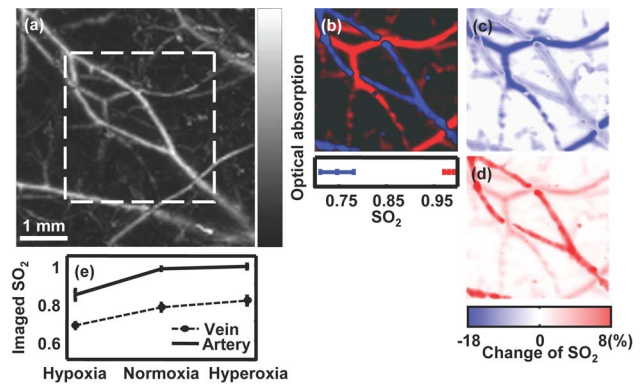

FIG. 2. (Color online) PAM imaging of variations in SO_2 in single subcutaneous blood vessels in a 200 g Sprague Dawley rat *in vivo*. (a) Structural image reflecting the total hemoglobin concentration acquired at the 584 nm optical wavelength under hyperoxia. (b) Static SO_2 image within the marked region in panel A under normoxia, where arteries and veins are pseudocolored red and blue, respectively, based on the imaged SO_2 values. (c) Image of the SO_2 changes from normoxia to hypoxia (hypoxia value—normoxia value). (d) Image of SO_2 changes from normoxia to hyperoxia (hyperoxia value—normoxia value). (e) Typical imaged values of SO_2 in venous and arterial bloods under all three physiological states, where different trends of variation are observed.

place $\mu_a(\lambda_i)$ by $\phi(\lambda_i, x, y, z)$ to calculate the [HbR] and (HbO$_2$) in relative values. Least-squares fitting gives

$$\begin{bmatrix} [\text{HbR}] \\ [\text{HbO}_2] \end{bmatrix}_{(x,y,z)} = (M^T M)^{-1} M^T \Phi(x,y,z) K, \qquad (2)$$

where

$$M = \begin{bmatrix} \varepsilon_{\text{HbR}}(\lambda_1) & \varepsilon_{\text{HbO}_2}(\lambda_1) \\ \vdots & \vdots \\ \varepsilon_{\text{HbR}}(\lambda_n) & \varepsilon_{\text{HbO}_2}(\lambda_n) \end{bmatrix}, \quad \Phi(x,y,z) = \begin{bmatrix} \phi(\lambda_1, x, y, z) \\ \vdots \\ \phi(\lambda_n, x, y, z) \end{bmatrix},$$

and K is the proportionality coefficient that is related to the ultrasonic parameters and the wavelength-dependent change of the local optical fluence as light passes through the skin.[15,16] Thus, the SO_2 image is calculated as

$$SO_{2(x,y,z)} = \frac{[\text{HbO}_2]_{(x,y,z)}}{[\text{HbO}_2]_{(x,y,z)} + [\text{HbR}]_{(x,y,z)}}. \qquad (3)$$

Due to the unknown coefficient K, only relative concentrations of the HbR and HbO$_2$ are calculated from Eq. (2). However, the SO_2 from Eq. (3) is absolute. Although two wavelengths are enough to determine SO_2 in principle, we used four wavelengths in all of our studies in order to reduce the influence of measurement error according to the theory of least-squares fitting.[17] The spectral region was between 570 and 600 nm and the published molar extinction coefficients[18,19] of HbR and HbO$_2$ were used.

In the phantom study, two ink samples (fiesta red and lake placid blue, Private Reserve Ink, IN) were mixed in various concentration ratios to mimic different levels of SO_2. By controlling the total concentration, the mixed samples had optical absorption coefficients comparable to that of blood. The four optical wavelengths in this study were 570, 580, 590, and 600 nm. During data collection, the mixed solution was injected into a transparent tube (TYGON S-54-HL, Norton Performance Plastics, NJ) with an inner diameter of 0.25 mm. The fraction of the red ink concentration in the total ink concentration, [red]/([red]+[blue]), was calculated using the peak PA amplitude, which matched the actual values with less than 1% error [Fig. 1(a)].

In the *ex vivo* study, venous bovine blood was freshly acquired and was mixed with an anticoagulant (citrate dextrose solution) before the experiment. Oxygenated and deoxygenated bloods were obtained by saturating the blood with pure oxygen and pure carbon dioxide,[19] respectively. Then, the fully oxygenated and deoxygenated bloods were mixed in different volumetric ratios to make samples of various SO_2 levels.[20] These samples were injected into the transparent tube and PAM measurements were made at four optical wavelengths: 578, 584, 590, and 596 nm. During the experiment, a slow and steady blood flow (~ 0.4 ml/h) in-

side the tube was maintained by an infusion pump (A-99, Braintree Scientific, MA). In addition to the PAM measurements, the SO_2 levels of these blood samples were also measured using a spectrophotometric method for comparison.[21] The mixed blood samples were first hemolyzed by adding 0.5% saponin. Then the optical absorption of each sample was measured by a spectrophotometer (GENESYS 20, Thermo Electron, MA) with near-infrared light (from 700 to 1000 nm with a step size of 4 nm) to calculate SO_2. These two independent calculations of SO_2 agreed with each other with a systematic difference of $\sim 4\%$ [Fig. 1(b)], which presumably came from the different readings of optical wavelengths in the two systems but could be compensated for by a system calibration.

In vivo data were collected on Sprague Dawley rats (~ 200 g, Charles River Breeding Laboratories, MA). All experimental animal procedures were carried out in conformity with the guidelines of the National Institutes of Health.[22] The laboratory animal protocol for this work was approved by university.

Before imaging, hair was removed from the back of the rats with a commercial human hair remover. A dose of 87 mg/kg ketamine, plus 13 mg/kg xylazine, was administered intramuscularly to anesthetize the rat and supplemental injections (~ 50 mg/kg h) minimized the rat's motion. During the experiment, the arterial blood oxygenation and the heart rate of the rat were monitored by a pulse oximeter (8600 V, Nonin Medical, MN). Three physiological states (hyperoxia, normoxia, and hypoxia) were introduced by controlling the oxygen concentration in the inhaled gases (pure oxygen, normal air, and carbogen consisting of 5% O_2, 5% CO_2, and 90% N_2). For each of the three states, PAM images were acquired to calculate the SO_2 at the same four wavelengths as in the ex vivo study.

Figure 2(a) shows the structural maximum-amplitude-projection (MAP) image,[6,9] which was acquired at the 584 nm wavelength, of subcutaneous vessels under hyperoxia. Since HbR and HbO$_2$ have identical molar extinction coefficients at this optical wavelength (isosbestic point), Fig. 2(a) reflects the total hemoglobin concentration distribution.

After images were acquired at all four different optical wavelengths at each physiological state, the [HbR] and [HbO_2] were first calculated on a point-by-point basis, and then the SO_2 was calculated within the blood vessels only, based on a vessel segmentation from Fig. 2(a). Because the SO_2 levels of venous and arterial bloods are physiologically distinctive, arteries and veins can be separated based on the imaged SO_2 values[9] as shown in Fig. 2(b). Consequently, dynamic variations in SO_2 between the physiological states were imaged on a vessel-by-vessel basis. Figures 2(c) and 2(d), respectively, show the differential MAP images of the SO_2 changes from normoxia to hypoxia and from normoxia to hyperoxia in single vessels. In this special case, the typical imaged values of SO_2 in venous and arterial bloods under all three physiological states are given in Fig. 2(e) for comparison. The imaged changes of SO_2 in the arterioles matched the oximeter readings and other published data.[23–25]

Based on anatomical observation, the imaged blood vessels were located beneath the dermis. The wavelength-dependent optical attenuation in the dermal layer must be considered in imaging SO_2. In this study, the measured PA amplitudes were compensated for by the average wavelength-dependent optical attenuation, which was acquired by measuring the PA amplitudes generated from a subcutaneously inserted black polyethylene film at different optical wavelengths. This average optical attenuation spectrum of the dermis has been shown not to change significantly with different imaging locations and animals.[15] The same compensation was applied to all of the three physiological states in order to assure that the imaged variations were caused only by real changes in the SO_2. However, the systematic change of SO_2 itself does affect optical attenuation in the skin. Thus, such compensation should be adjusted for different physiological states accordingly to achieve a more precise quantitative measurement.

The *in vivo* experiment demonstrated the unique feature of PAM, the ability to image SO_2 with high spatial resolution, high sensitivity, and high specificity in single vessels. In some tumor angiogenesis imaging, PAM can be used to observe both the morphology of newly grown vessels and the oxygen consumption of a tumor at different stages. It can also be used to evaluate the effect of certain tumor treatments since tumor hypoxia is the primary resistance to therapeutic methods. In wound healing imaging, PAM can be used to monitor tissue regeneration, which is accompanied by higher SO_2 levels as well as the formation of new blood vessels. Another important application of PAM is the imaging of brain functions in response to sensory stimulations. It has been observed that sensory stimulations result in a quick drop followed by a gradual increase of oxygenation that usually lasts several seconds in the corresponding brain cortex.[1] Since PAM acquires one *A* line within a few microseconds, it can provide high temporal resolution in SO_2 imaging for time-course studies. Moreover, because the thickness of the brain cortex is more than 1.5 mm,[26] PAM has an advantage over the existing optical method[1] due to its large imaging depth.

In summary, PAM has been used to image the variations in blood oxygenation in single vessels *in vivo* under three physiological states with high spatial resolution and high sensitivity. . Because the current imaging speed is limited only by the laser pulse rate (10 Hz), a higher repetition rate laser will significantly reduce the data acquisition time.

[1] I. Vanzetta and A. Grinvald, Science **286**, 1555 (1999).

[2] C. Chandrakala and D. L. Fraker, Cancer Lett. **211**, 225 (2005).

[3] A. A. Tandara and T. A. Mustoe, World J. Surg. **28**, 294 (2004).

[4] S. S. Foo, D. F. Abbott, N. Lawrentschuk, and A. M. Scott, Mol. Imaging Biol. **6**, 291 (2004).

[5] E. V. Savateeva, A. A. Karabutov, B. Bell, R. Johnigan, M. Motamedi, and A. A. Oraevsky, Proc. SPIE **3916**, 55 (2000).

[6] H. F. Zhang, K. Maslov, M.-L. Li, G. Stoica, and L. V. Wang, Opt. Express **14**, 9317 (2006).

[7] K. Maslov, G. Stoica, and L. V. Wang, Opt. Lett. **30**, 625 (2005).

[8] H. F. Zhang, K. Maslov, G. Stoica, and L. V. Wang, J. Biomed. Opt. **11**, 054033 (2006).

[9] H. F. Zhang, K. Maslov, G. Stoica, and L. V. Wang, Nat. Biotechnol. **24**, 848 (2006).

[10] G. J. Diebold, M. I. Khan, and S. M. Park, Science **250**, 101 (1990).

[11] A. C. Tam, Rev. Mod. Phys. **58**, 381 (1986).

[12] R. A. Kruger, P. Liu, Y. R. Fang, and C. R. Appledorn, Med. Phys. **22**, 1605 (1995).

[13] X. Wang, Y. Pang, G. Ku, X. Xie, G. Stoica, and L. V. Wang, Nat. Biotechnol. **21**, 803 (2003).

[14] B. Chance, E. Borer, A. Evans, G. Holtom, J. Kent, M. Maris, K. Mccully, J. Northrop, and M. Shinkwin, Ann. N.Y. Acad. Sci. **551**, 1 (1988).

[15] K. Maslov, M. Sivaramakrishnan, H. F. Zhang, G. Stoica, and L. V. Wang, Proc. SPIE **6086**, 215 (2006).

[16] X. Wang, X. Xie, G. Ku, L. V. Wang, and G. Stoica, J. Biomed. Opt. **11**, 024015 (2006).

[17] A. C. Tamhane and D. D. Dunlop, *Statistics and Data Analysis: From Elementary to Intermediate* (Prentice-Hall, Englewood Cliffs, NJ, 2000), p. 408.

[18] S. L. Jacques and S. A. Prahl, *Absorption Spectra for Biological Tissues* (Oregon Medical Laser Center, OR, 2004), http://omlc./ogi.edu/spectra/hemoglobin/index.html

[19] W. G. Zijlstra, A. Buursma, and O. W. van Assendelft, *Visible and Near Infrared Absorption Spectra of Human and Animal Hemoglobin, Determination and Application* (VSP, Amsterdam, The Netherlands, 2000).

[20] P. Scheid and M. Meyer, J. Appl. Physiol. **45**, 818 (1978).

[21] M. Tsao, S. Sethna, C. Sloan, and L. Wyngarden, J. Biol. Chem. **217**, 479 (1955).

[22] National Institutes of Health Publication No. 86-23 (U.S. GPO, Washington, DC, 1985).

[23] S. Kety and C. Schmidt, J. Clin. Invest. **27**, 484 (1948).

[24] T. Duong, C. Iadecola, and S. Kim, Magn. Reson. Med. **45**, 61 (2001).

[25] T. Yoshida, M. Udo, M. Chida, M. Ichioka, and K. Makiguchi, Eur. J. Appl. Physiol. **58**, 772 (1989).

[26] E. Sowell, P. Thompson, C. Leonard, S. Welcome, E. Kan, and A. Toga, J. Neurosci. **24**, 8223 (2004).